Euler-Lagrange coupling for porous parachute canopy analysis

Nicolas Aquelet[*], Benjamin Tutt[**]
[*]Livermore Software Technology Corp., 7374 Las Positas Road,
Livermore, CA 94551
aquelet@lstc.com
[**]Irvin Aerospace Inc,Santa Ana,CA 92704
BTutt@irvinaerospace.com

ABSTRACT
We apply a new Euler-Lagrange coupling method to 3-D parachute problems, which generally involve fluid-structure interactions between a flexible, elastic, porous parachute canopy and a high-speed airflow. The method presented couples an Arbitrary Lagrange Euler formulation for the fluid dynamics and an updated Lagrangian finite element formulation for the parachute canopy. The Euler-Lagrange coupling handles fluid-structure interaction without matching the fluid and structure meshes. In order to take account of the effect of the parachute permeability, this coupling computes interaction forces based on the Ergun porous flow model. This paper provides validations for the technique when considering parachute applications and discusses the interest of this development to the parachute designer.

Keywords: Euler-Lagrange coupling, porous canopy, Ergun equation, ALE[1] formulation, fluid-structure interaction

INTRODUCTION

The parachute design needs to take account of four phases in the airdrop: deployment, inflation, terminal descent and impact.

The deployment depends on how the parachute is packed into the bag. It also depends on the pilot which is a small parachute deployed first to pull the main parachute out of the bag. Another way of deploying a parachute directly after leaving the aircraft is the static line.

The second phase begins as soon as the parachute canopy is pulled free from the deployment bag. When air flows into the canopy, the major part is trapped which increases the pressure differential and inflates the canopy. The remaining part of air that enters the parachute canopy flows out through the vent, the gaps between the ribbons and the natural porosity of the fabric. Two forms of porosity are considered in parachute design: geometric porosity and fabric permeability. Geometric porosity is defined as the ratio of all open areas or physical gaps to the total canopy area. Fabric air-permeability is defined as the airflow through the canopy cloth in CFM/ft^2 (cubic feet per minute per square foot = 0.00508m/s),

[1] Arbitrary Lagrange Euler

at ½ inch water pressure (=0.249082kPa). When considering parachutes consisting of both geometric porosity and fabric permeability, a term referred to as equivalent porosity is often used. The Space Shuttle Orbiter landing-brake parachute, and fighter aircraft spin/stall recovery parachutes, see Figure 1, are examples of parachutes containing high geometric porosity.

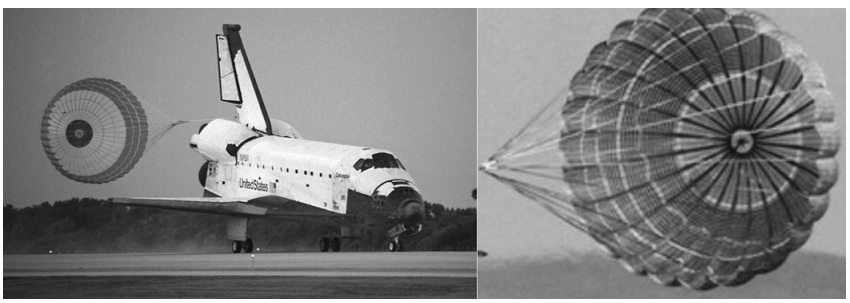

Figure 1 Parachutes Exhibiting High Geometric Porosity

Parachute porosity, whether geometric or permeability based is an important matter in the design of a parachute canopy. It affects drag performance, stability and opening forces. Parachute drag performance, maximum oscillation angle, and opening forces all reduce with increasing porosity. In the majority of applications, the reduction in stability and opening forces is advantageous but the decrease in drag is not. Further, a parachute that is too porous will not open at all. The substitution of an impervious material with a highly permeable fabric can turn a parachute from a wandering sloth into a plummeting stabilizer. An accurate consideration of fabric permeability has long eluded the parachute designer. The permeability of the canopy is devised to limit the "wake recontact phenomenon" or better known as "canopy collapse". Spahr & Wolf [1] first discussed the phenomenon of wake recontact using wake momentum considerations. They noticed that if the deceleration of the canopy is too important, the axial velocities in the wake region may be much larger than the parachute velocity, thus allowing the wake to catch up and collapse the parachute. Consequently, blowing through a porous fabric to push the wake away is important to prevent the parachute from collapsing.

After the inflation process is over, the parachute drops vertically at a speed determined by the payload weight and the parachute drag characteristics. Terminal descent is close to a steady-state process and the numerical applications in this paper focus on this phase, for which experimental results are available in the database of Irvin Aerospace. The last phase, the impact, is not studied in this paper.

The numerical simulation of the porous parachute problem is a complex fluid-structure interaction phenomenon. To appropriately simulate, and therefore understand and predict, this behavior requires an accurate method of assessing this complex relationship. Analysis of a parachute or a flow field without its associated partner is excluding the inherent interaction between the two. A general parachute code that can accurately predict three-dimensional FSI

for various parachute systems under the different stages described previously was developed by T*AFSM (Team for Advanced Flow Simulation and Modeling) [2][3][4]. However, in these approaches, the canopies were impermeable. In the literature, the canopy permeability in the computation of the fluid-structure interaction can be taken into account

by vortex element methods [5][6] and grid-based models like the immersed boundary methods [7] [8] [9] or the Euler-Lagrange coupling formulation [10][11], which was chosen to carry out the study in this paper.

The first method places vortex elements in regions, where vorticity has been shed from the canopy surface. These vortex are usually convected, stretched, and diffused in the flow by solving the vorticity-transport equation derived from the rotational of the Navier-Stokes momentum equation. Strickland [12] implemented, in a code named VPARA, a vortex method solving the flow field over axisymmetric bluff bodies. Using this code, Higuchi et al [13] modeled the flow behind an accelerating and decelerating disk. In the case of severe decelerations, the wake rapidly overtook the disk what involved an important reduction of the drag force; this force could even be negative. Sarpkaya et al. [14] investigated the effects of the porosity on the wake recontact, through the use of the vortex element method. However the structure in this study was rigid. For solving the fluid-structure interaction problem other investigations couples the vortex methods to a finite element method for the canopy.

Sundberg [15] successfully coupled the VPARA code [12] with the structural dynamics code PRONTO2D [16]. Later a similar code, VIPAR [17] (Vortex Inflation Parachute), was fully coupled to a structural dynamics code for predicting flow past deformable bluff structure. During the terminal descent the vortex element method accurately models the wake behind the parachute. However a final model for routine design work should be able to perform complete numerical simulations of parachute deployment, inflation, and steady descent. An ALE formulation [18][19] can handle the deployment process, which involves, in most cases, a fast-transient and unsteady fluid-structure interaction problem whereas the vortex element method is not designed for this purpose. This method supposes also a divergence-free flow but in some parachute applications [20] the Mach number can be enough high to call the assumption of an incompressible flow in question.

In the grid-based models, the immersed boundary method [7] [8] assumes also an incompressible flow and the numerical approach is based on a finite difference discretization of the Navier-Stokes equations. The canopy is a massless boundary required to move at the local fluid velocity, which takes account of the flux through the pores of the canopy. To compute the inertia effect of the parachute, the massless boundary is related to a massive boundary by penalty springs [9]. In this formulation, the action of the elastic canopy on the fluid is a local body force in the Navier-Stokes momentum equation. A Darcy's law computes the body force. Actually the method proposed in this paper is close to the immersed boundary method. The parachute meshed by Lagrangian finite elements is also immersed in an ALE grid, which modeled the air fluid flow. However this latter is not supposed divergence-free. The fluid-structure interaction force computed by an Euler-Lagrange coupling is based on a law close to the Darcy's one, the Ergun equation [21]. A description of the method employed in this paper is detailed in the following parts. First the governing equations for the fluid and parachute problems are formulated together with boundary conditions. Then a description of the porous Euler-Lagrange coupling algorithm is presented. Further, this numerical method is validated by several porous parachute applications with a comparison to experimental data.

2. DESCRIPTION OF THE FLUID AND STRUCTURE PROBLEMS

The fluid is solved by using an Eulerian formulation [22] on a Cartesian grid that overlaps the porous structure, while this latter is discretised by Lagrangian shells based on the Belytschko-Lin-Tsay formulation [23] . The equations in the following paragraphs are based

on the Farhat's formalism [19], which divides the coupled problem in three fields : the fluid, the structure and the mesh.

2.1. EULERIAN DESCRIPTION OF NAVIER-STOKES EQUATIONS

For simplicity, the numerical simulations in this paper have been restricted to an Eulerian formulation for the fluid, although the formulation can be extended to an ALE formulation. The Eulerian formulation is a particular case of the ALE finite element formulation. Thus a general ALE point of view is first adopted to solve the Navier-Stokes equations before presenting the Eulerian formulation.

In the ALE description of motion, an arbitrary referential coordinate is introduced in addition to the Lagrangian and Eulerian coordinates [24], [25]. The total time derivative of a variable f with respect to a reference coordinate can be described as Eqn.(1):

$$\frac{df(\vec{X},t)}{dt} = \frac{\partial f(\vec{x},t)}{\partial t} + (\vec{v} - \vec{w}).\overrightarrow{grad} f(\vec{x},t) \tag{1}$$

where $\vec{X}$ is the Lagrangian coordinate, $\vec{x}$ is the ALE coordinate, $\vec{v}$ is the particle velocity and $\vec{w}$ is the velocity of the reference coordinate, which will represent the grid velocity for the numerical simulation, and the system of reference will be later the ALE grid. Thus substituting the relationship between the total time derivative and the reference configuration time derivative derives the ALE equations.

Let $\Omega^f \epsilon R^3$, represent the domain occupied by the fluid, and let $\partial\Omega^f$ denote its boundary. The equations of mass, momentum and energy conservation for a Newtonian fluid in ALE formulation in the reference domain, are given by:

$$\frac{\partial \rho}{\partial t} + \rho div(\vec{v}) + (\vec{v} - \vec{w}) grad(\rho) = 0 \tag{2}$$

$$\rho \frac{\partial \vec{v}}{\partial t} + \rho(\vec{v} - \vec{w}).\overline{\overline{grad}}(\vec{v}) = \overrightarrow{div}(\overline{\overline{\sigma}}) + \vec{f} \tag{3}$$

$$\rho \frac{\partial e}{\partial t} + \rho(\vec{v} - \vec{w}).\overrightarrow{grad}(e) = \overline{\overline{\sigma}} : \overline{\overline{grad}}(\vec{v}) + \vec{f}.\vec{v} \tag{4}$$

where ρ is the density and $\overline{\overline{\sigma}}$ is the total Cauchy stress given by:

$$\overline{\overline{\sigma}} = -P.\overline{\overline{Id}} + \mu(\overline{\overline{grad}}(\vec{v}) + \overline{\overline{grad}}(\vec{v})^T) \tag{5}$$

where p is the pressure and μ is the dynamic viscosity. Equations (2)-(4) are completed with appropriate boundary conditions. The part of the boundary at which the velocity is assumed to be specified is denoted by $\partial\Omega^f_1$. The inflow boundary condition is:

$$\vec{v} = \vec{g}(t) \quad on \quad \partial\Omega_1^f \tag{6}$$

The traction boundary condition associated with Eqn.(4) are the conditions on stress components. These conditions are assumed to be imposed on the remaining part of the boundary.

$$\overline{\overline{\sigma}}.\vec{n} = \vec{h}(t) \quad on \quad \partial\Omega_2^f \tag{7}$$

One of the major difficulties in time integration of the ALE Navier-Stokes equations (2)-(4) is due to the nonlinear term related to the relative velocity ($\vec{v} - \vec{w}$). For some ALE formulations, the mesh velocity can be solved using a remeshing and smoothing process. In the Eulerian formulation, the mesh velocity $\vec{w} = \vec{0}$, this assumption eliminates the remeshing and smoothing process, but does not simplify the Navier-Stokes equations (2)-(4). To solve equations (2)-(4), the split approach detailed in [22], [24] and implemented in most hydrocodes such as LS-DYNA® is adopted in this paper. Operator splitting is a convenient method for breaking complicated problems into series of less complicated problems. In this approach, first a Lagrangian phase is performed, using an explicit finite element method, in which the mesh moves with the fluid particle. In the CFD community, this phase is referred to as a linear Stokes problem. In this phase, the changes in velocity, pressure and internal energy due to external and internal forces are computed. The equilibrium equations for the Lagrangian phase are:

$$\rho\frac{d\vec{v}}{dt} = \overrightarrow{div}(\overline{\overline{\sigma}}) + \vec{f} \tag{8}$$

$$\rho\frac{de}{dt} = \overline{\overline{\sigma}} : \overline{\overline{grad}}(\vec{v}) + \vec{f}.\vec{v} \tag{9}$$

The mass conservation equation is used in its integrated form Eqn.(10) rather than as a partial differential equation [26]. Although the continuity equation can be used to obtain the density in a Lagrangian formulation, it is simpler and more accurate to use the integrated form Eqn.(10) in order to compute the current density ρ:

$$\rho J = \rho_0 \tag{10}$$

where ρ_0 is the initial density and J is the volumetric strain given by the Jacobian:

$$J = \det\left(\frac{\partial x_i}{\partial X_j}\right) \tag{11}$$

In the second phase, called advection or transport phase, the transportation of mass, momentum and energy across element boundaries are computed. This may be thought of as remapping the displaced mesh at the Lagrangian phase back to its initial position. The transport equations for the advection phase are:

$$\frac{\partial \phi}{\partial t} + \vec{c}.\overrightarrow{grad}(\phi) = 0$$
$$\phi(\vec{x},0) = \phi_0(x) \tag{12}$$

where $\vec{c} = \vec{v} - \vec{w}$ is the difference between the fluid velocity $\vec{v}$, and the velocity of the computational domain $\vec{w}$, which will represent the mesh velocity in the finite element formulation. In some papers [22], [26] $\vec{c}$ is referred as the convective velocity. The hyperbolic equation system (12) is solved by using a finite volume method. Either a first order upwind method or second order Van Leer advection algorithm [27] can be used to solve Eqn.(12). The advection method is successively applied for the conservative variables: mass, momentum and energy with initial condition ϕ_0(x), which is the solution from the Lagrangian calculation of equations (8)-(9) at the current time. In Eqn.(12), the time *t* is a fictitious time: in this paper, time step is not updated when solving for the transport equation. There are different ways of splitting the Navier-Stokes problems. In some split methods, each of the Stokes problem and transport equation are solved successively for half time step. The following paragraph presents the description of the structure.

2.2. LAGRANGIAN DESCRIPTION OF THE POROUS CANOPY

In this paragraph the porous structure problem is described at the macroscopic scale and the Belytschko-Lin-Tsay shell formulation [23] employed to model the thin porous medium is compared to the Hughes Liu shell formulation [28].

Let $\Omega^s \epsilon R^3$, the domain occupied by the porous structure, and let $\partial\Omega^s$ denote its boundary. An updated Lagrangian finite element formulation is considered: the movement of the thin porous medium Ω^s described by x_i (t),$(i = 1,2,3)$ can be expressed in terms of the reference coordinates Xi (t),$(i = 1,2,3)$ and time t:

$$x_i = x_i(X_\alpha, t) \tag{13}$$

The momentum equation is given by Eqn.(16) in which $\bar{\bar{\sigma}}$ is the Cauchy stress, ρ is the density, f is the force density, $\frac{d\vec{v}}{dt}$ is acceleration and $\vec{n}$ is the unit normal oriented outward

at the boundary $\partial\Omega^s$:

$$\rho\frac{d\vec{v}}{dt} = \overrightarrow{div}(\bar{\bar{\sigma}}) + \vec{f} \tag{14}$$

$$\rho\frac{de}{dt} = \bar{\bar{\sigma}} : \overrightarrow{\overrightarrow{grad}}(\vec{v}) + \vec{f}.\vec{v} \tag{15}$$

The solution of Eqn.(14)-(15) satisfies the displacement boundary condition Eqn.(16) on the boundary $\partial\Omega_1^s$ and the traction boundary condition Eqn.(17) on the boundary $\partial\Omega_2^s$.

$$\rho\frac{de}{dt} = \overline{\overline{\sigma}} : \overline{\overline{grad}}(\vec{v}) + \vec{f}.\vec{v} \tag{15}$$

$$\vec{x}(\vec{X},t) = \vec{D}(t) \text{ on } \partial\Omega_1^s \tag{16}$$

In this paper, the shell formulation used to model the parachute canopy is the Belytschko-Lin-Tsay formulation [17]. The Belytschko-Lin-Tsay shell 4-node element is based on a co-rotational coordinate system and a constitutive computation using a rate of deformation. The embedded element coordinate system that deforms with the element is defined in term of four corner nodes. As the element deforms, an angle may exist between the fiber direction and the unit normal of the element coordinate system. The magnitude of this angle is limited in order to keep a plane shell geometry. In this local system, the Reissner-Mindlin theory gives the velocity of any point in the shell according to the velocity of mid-surface and the rotations of the element's fibers. Then the rates of deformation are computed at the center of the element. The new Cauchy stresses are computed by using the material model and by accounting for the incremental rotation, $\Delta\overline{\overline{R}}$.

For the Hughes-Liu family of shell elements [28], $\Delta\overline{\overline{R}}$ is estimated by using an approximation of the Jaumann rate. Therefore, in every integration points, the instantaneous rotation field is computed. Moreover, since the Jaumann rate update is performed in the global system, the stresses and the rates of deformations are rotated from the global coordinate system to the local coordinate system and, after the update, the new stresses are rotated back to the global system. Thus, the Jaumann rate rotation requires the most operation cost in the Hughes-Liu shell process. For the Belytschko family of elements, the incremental rotation is obtained by expressing the element base vectors at t(n+1) in the local system at t(n). Since the material rotation is equal to the rotation of the local system, $\Delta\overline{\overline{R}}$ is the identity matrix. This involves the Belytschko-Lin-Tsay shell element is a computationally efficient alternative to the Hughes-Liu shell element. Then, the element-centered resultant forces and moments are obtained by integrating the stresses through the thickness of the shell. The relations between these forces and moments and the local nodal forces and moments are obtained by performing the principle of virtual power with one point quadrature. Finally, the global nodal forces and moments are derived by using the transformation relations defined by the global components of the corotational unit vectors. The following section presents the porous Euler-Lagrange coupling method, which handles the fluid - porous structure problem.

3. FLUID-STRUCTURE INTERACTION

The Lagrangian finite element formulation uses a computational mesh that follows the material deformation. This approach is efficient and accurate for problems involving moderate deformations like structure motions or flows that are essentially smooth. When this latter departs from this kind of smoothness, the ALE or Eulerian formulation must be used because the finite element mesh is independent from the material flow. This takes away all problems associated with distorted mesh that are commonly encountered with a Lagrangian approach. In this paper the Euler Lagrange coupling using a Eulerian formulation for the

fluid, is more suitable for solving parachute problems and more generally, fast transient porous fluid-structure interaction problems. First, the Eulerian formulation is able to simulate fluid large deformations and second, the coupling can handle the interaction between the fluid and thin porous medium. This method can be described as Eulerian contact. The following paragraph presents the principle of the coupling .

3.1. POROUS EULER-LAGRANGE COUPLING

In an explicit time integration problem, the main part of the procedure in the time step is the calculation of the nodal forces. After computation of fluid and structure nodal forces, we compute the forces due to the coupling, these will only affect nodes that are on the fluid - porous structure interface. For each structure node, a depth penetration $\vec{d}$ is incrementally updated at each time step, using the relative velocity v_{rel} at the slave and master node. For this coupling, the slave node is a structure mesh node, whereas the master node is not a fluid mesh node, it can be viewed as a fluid particle within a fluid element, with mass and velocity interpolated from the fluid element nodes using finite element shape functions. The location of the master node is also computed using the isoparametric coordinates of the fluid element. If $\vec{d}^n$ represents the penetration depth at time , it is incrementally updated in Eqn.(18):

$$\vec{d}^{n+1} = \vec{d}^{n} + \overrightarrow{v_{rel}}^{n+1/2}.\Delta t \tag{18}$$

In Eqn.(18) $\overrightarrow{v_{rel}}^{n+1/2} = \vec{v}_s^{n+1/2} - \vec{v}_f^{n+1/2}$ in which the fluid velocity $\vec{v_f}$ is the velocity at the master node location and the structure velocity $\vec{v_s}$ is the velocity at the slave node location. The coupling acts only if penetration occurs, $\vec{n_s}.\vec{d}^{n} < 0$, where $\vec{n_s}$, where is built up by averaging normals of structure elements connected to the structure node. The porous coupling forces are derived from the integration of the Ergun Equation (Ergun, 1952) on the shell volume:

$$\frac{dp}{d\hat{z}} = a(\mu,\varepsilon)\overrightarrow{v_{rel}}.\vec{n_s} + b(\rho,\varepsilon)\left(\overrightarrow{v_{rel}}.\vec{n_s}\right)^2 \tag{19}$$

in which $\hat{z}$ is the local position along the fiber direction of the shell element and is the porosity: .

$$\varepsilon = \frac{v_{void}}{v_{total}}.$$

μ and ρ are the dynamic viscosity and density, respectively. The coefficient $a(\mu,\varepsilon)$is the reciprocal permeability of the porous shell or viscous coefficient. $b(\rho,\varepsilon)$ represents the inertia coefficient. For flows under very viscous conditions the second term in Eqn.(19), which represents the inertia effects drops out and the Blake-Kozeny equation for laminar flows in porous media is obtained. At high rates of flow it is the first term or viscous term, which drops out and the Blurke-Plummer equation for turbulent flows in porous media is obtained. For the parachute application the inertia effects should be preponderant. These coefficients can be derived from the Ergun theory:

$$a = \frac{150\mu(1-\varepsilon)^2}{D^2\varepsilon^3} \tag{20}$$

$$b = \frac{1.75\rho(1-\varepsilon)}{D\varepsilon^3} \tag{21}$$

D is a characteristic length defined by: $D = \frac{6(1-\varepsilon)V}{S}$ with V, the volume of the canopy and S, the "wetted" surface

The Ergun equation describes the magnitude of porous flow velocity at a given differential pressure based upon two coefficients. These coefficients assume a constant porosity, not to be confused with a constant permeability. Porosity is a characteristic of the fabric, whereas permeability is a description of the flow velocity at a given condition. Many materials can be highly porous without being permeable. It should also be noted that the porosity of some fabrics can change significantly with applied load but in the applications of this paper, a constant and uniform porosity is assumed. Figure 2 displays historical permeability data [29] of a common parachute cloth fabric, of particular interest is the widely used MIL-C-7020 Type III.

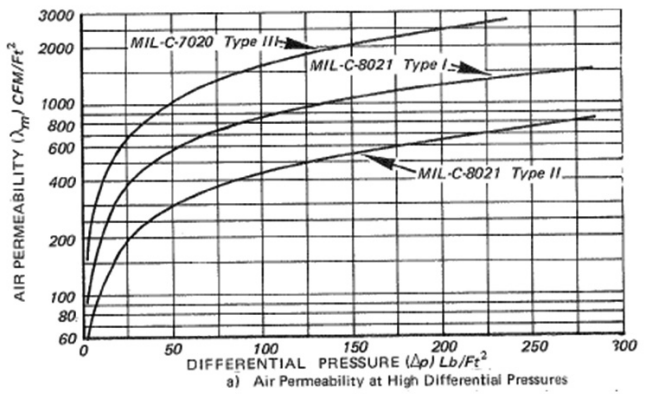

Figure 2 Parachute Fabric Permeability Data [23]

The data shown in Figure 2 was obtained at constant porosity, fluid viscosity and density. Under these assumptions the viscous and inertia parameters in Eqn.(19) are constant. To determine these coefficients, the Ergun theoretical permeability should be a parabolic fit of the experimental one. Thus the coefficients were computed by solving the following system:

$$\begin{cases} dp_1 / e = a.v_1 + b.v_1^2 \\ dp_2 / e = a.v_2 + b.v_2^2 \end{cases} \tag{22}$$

where e is the shell thickness and the couple of points (v_1, dp_1) and (v_2, dp_2) was chosen on so that the Ergun equation fits the experimental plot as close as possible.

The force F derived from Eqn.(19) is applied to both master and slave nodes in opposite directions to satisfy force equilibrium at the interface coupling, and thus the coupling is consistent with the fluid-structure interface condition namely the action-reaction principle. At the structure coupling node, we applied a force:

$$F_s = -F \tag{23}$$

whereas for the fluid, the porous coupling force is distributed to the fluid element nodes based on the shape functions, at each node i (i=1,..,8), the fluid force is scaled by the shape function N_i :

$$F_f^i = N_i.F \tag{24}$$

where N_i is the shape function at node i. Since $\sum_{i=1}^{8} F_f^i = F$, the action-reaction principle is satisfied at the coupling interface.

This conservative load projection was described by Farhat et al. [19]. The following paragraph presents the application of this approach to a porous disk parachute in terminal descent.

3.2. MODEL TEST

A simple model was constructed to validate the method of coefficient selection and evaluate the interpretation of the Ergun equation. Figure 3 illustrates a model containing two fluid elements with a porous shell, for which the fabric is the MIL-C-7020 type. A constant pressure was maintained in each solid element producing a constant differential pressure across the fabric boundary. The experimental data presented in Figure 2 were then compared with the flow velocities predicted in the model.

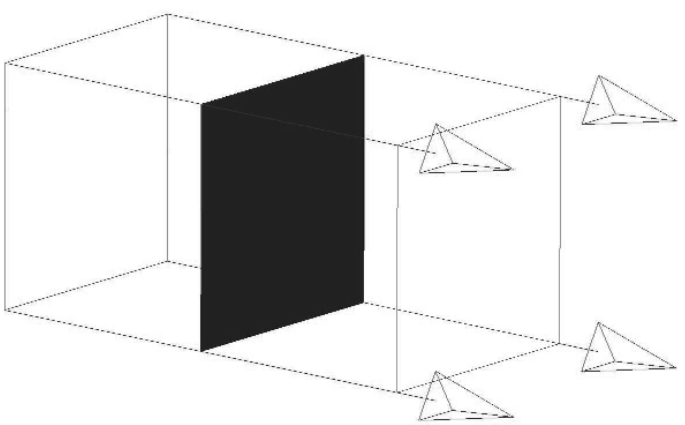

Figure 3 Permeability Coefficient Validation Model

The range of differential pressures over which the coefficients are effective was also assessed. Table 1 presents a comparison of experimental and simulation porous flow velocity over a range of differential pressures, 1197.41-10776.74 Pa (25-225 lb/ft^2).

Table 1: Comparison of Experimental and Numerical Porous Flow Velocity

Differential Pressure		**Experimental Velocity**		**Numerical Velocity**		**Relative Error**
Pa	lb/ft2	m/s	ft/s	m/s	ft/s	(%)
1197.41	25	201.17	660	208.79	685	3.6
2394.83	50	320.04	1050	329.18	1080	2.8
3592.25	75	426.72	1400	422.15	1385	1.1
4789.66	100	502.92	1650	501.40	1645	0.3
5987.08	125	563.88	1850	571.50	1875	1.3
7184.49	150	624.84	2050	635.51	2085	1.7
8381.91	175	685.80	2250	694.94	2280	1.3
9579.32	200	746.76	2450	749.81	2460	0.4
10776.74	225	807.72	2650	801.62	2630	0.8

The relative errors are within acceptable limits. It should be noted that similar validation methods were performed for various fabrics over a variety of differential pressures, all with similar success. Experimental data pertaining to MIL-C-7020 Type III was the most extensive and reliable and for these reasons has been included in this paper

4. NUMERICAL APPLICATIONS

4.1. SIMULATION METHODOLOGY

Before the development of the porous Euler-Lagrange coupling it was possible to analyze the parachute problem. A penalty Euler-Lagrange coupling algorithm permitted the interaction of the Eulerian formulation for the flow field, and the Lagrangian formulation for the parachute. Similarly to penalty contact algorithm [30], the coupling force in Eqns.(23-24) for the penalty Euler-Lagrange coupling is given by:

$$F = k.d \tag{25}$$

where k represents the spring stiffness, and d the penetration computed by Eqn.(18). The penalty Euler-Lagrange coupling was applied with the following methodology for parachute performance predictions at Irvin:

- Model the parachute using a Lagrangian formulation.
- Model the fluid domain using a Navier-Stokes based Eulerian formulation.
- Perform the analyses using conditions similar to a wind tunnel, i.e. infinite mass flow; equating the results to the quasi-steady-descent phase of the parachute flight.

The last step reduced the computational cost associated with modeling vast spatial timelines associated with real parachute functions, specifically deployment and inflation. It also permitted the reduction in complexity of boundary conditions. Irvin developed this methodology several years ago and it has yielded excellent results for a number of parachutes with a low-permeability fabric. Tutt [31] has previously published data that described the use of the penalty coupling to simulate the parachute behavior. This work discussed the benefit of visualizing the flying shape and anticipating the performance of a newly designed tactical

mass assault troop parachute, prior to fabrication and testing. Particularly noteworthy is the replication of an undesirable flight characteristic exhibited by a replacement candidate for the venerable T-10 mass tactical assault parachute. The identification, and subsequent removal, of this flight mode through simulation design iterations demonstrated the powerful potential of such techniques. The modified version of that parachute system is now undergoing operational testing and will replace the T-10 later in this decade. Figure 4 illustrates a flight test with simulation flow field velocity vectors overlaid. The fabric shown in Figure 4 is classified as a low-permeability fabric. When assessing the steady state characteristics of this parachute the approximation of an impermeable fabric was valid. Minimal differential pressure is developed across the canopy when a constant rate of descent is achieved.

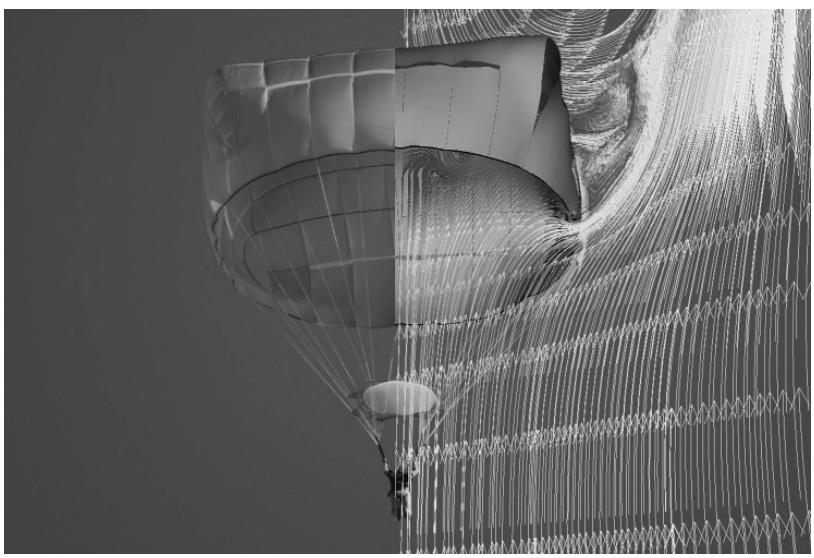

Figure 4 Flight Test and Simulation Comparison

However the study of Tutt [31] exposed also the inability to consider fabric permeability as an authentic limitation that would restrict the application of the methodology for a number of applications. To circumvent this drawback the porous Euler-Lagrange coupling was developed and it now replaces the penalty coupling in the previous methodology. The following paragraph compares the two coupling method and shows the limits of the penalty coupling in solving parachute problems with a high-permeable canopy fabric.

4.2. PARACHUTE SIMULATION

A pertinent example of a parachute design that could not accurately be assessed using the penalty Euler-Lagrange coupling is the TP8 low altitude troop parachute. The TP8 is an aeroconical class of parachute. Aeroconical parachutes are commonly used for aircrew ejection systems. The TP8, shown in Figure 5, is fabricated from two base cloths of different permeability. The crown of the canopy is constructed from cloth exhibiting a permeability of 0.0508m/s (10 CFM/ft^2), and the major part of the skirt is rated at 0.4064m/s (80 CFM/ft^2), both at ½ inch water pressure.

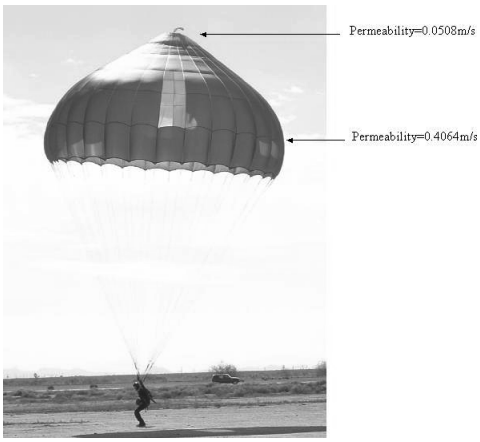

Figure 5 TP8 Flight Test

Drag coefficient, C_d, is widely used as a measure of parachute performance and is defined:

$$\frac{dp}{d\hat{z}} = a(\mu,\varepsilon)\overrightarrow{v_{rel}}.\overrightarrow{n_s} + b(\rho,\varepsilon)\left(\overrightarrow{v_{rel}}.\overrightarrow{n_s}\right)^2 \tag{19}$$

where F_D is the drag force, S_0 canopy surface area and V is the velocity at the inlet of the channel.

Test data indicates that the TP8 exhibits a drag coefficient of approximately 0.6.

A constant flow rate with a velocity of 5.486 m/s (18 ft/s), which equates to the steady rate of descent in an actual flight test is applied to the inlet of the wind tunnel modeled by an Eulerian grid with 8-node elements ranging from 0.05m (2in) to 2m (80in). Initial and boundary conditions reflect a wind tunnel conditions. Sliding conditions are applied on the lateral boundaries of the Eulerian grid. The parachute is modeled by a Lagrangian formulation. The canopy is meshed with 4-node Belytschko-Lin-Tsay [23] shell elements ranging from 0.13m (5in) to 0.26m (10in).

Two different simulations are compared with the experimental test:

- In the first modeling, the fluid-structure interaction is handled by a penalty Euler-Lagrange coupling and,
- In the second one, the fluid-structure interaction problem is solved with a porous Euler-Lagrange coupling.

With a time step of 0.05ms, the number of cycles to conduct the simulation is around 200.000. It takes 220h to complete on a single 32bit Intel Xeon® machine. Instabilities could occur for a time step too large. The CFL time step is actually scaled down to prevent the run from the crash. It has been noticed that the higher the inflow velocity is, the lighter the fabric is, and the lower the time step should be.

Figure 6 provides time history data of the drag force produced by the canopy when subjected to a flow velocity of 5.486 m/s (18 ft/s). On this figure, the coupling force time history reaches the steady state after 9s. The drag coefficient is computed after this time. The penalty coupling predicts a drag coefficient of 0.75. Clearly, this prediction is in conflict with

the experimental value of 0.6, a value derived from a significant and reliable test series. The assumption of an impervious canopy cloth is the obvious factor in the difference between test and simulation results. Figure 7 presents a qualitative assessment of the permeability affect. It illustrates a cross-section of flow velocity for the TP8 simulation with and without accounting for fabric permeability. This figure presents an excellent illustration of the influence of fabric permeability in parachute design. The porous flow through the canopy cloth has completely changed the nature of the parachute wake. The large recirculation of air behind the parachute remains very close to the canopy on the left and has a significant effect on the parachute stability. By permitting air to flow through the canopy, the recirculating air has been pushed further downstream where it has considerably less influence on the stability of the parachute. Thus the "wake recontact phenomenon", which may cause the parachute collapse, is clearly prevented. This results in a discernible difference in drag coefficient. Figure 6 gives also a quantitative comparison of the same simulation with and without permeability. The data clearly depicts the reduction in drag associated with the incorporation of permeability. Also noticeable is the reduction in numerical noise, this is associated with a more benign parachute inflation, a characteristic of porous canopies. The steady-state drag force from Figure 7 can be used to calculate a modified drag coefficient; the simulation now predicts a C_d of 0.59, which is close to the experimental value: 0.6.

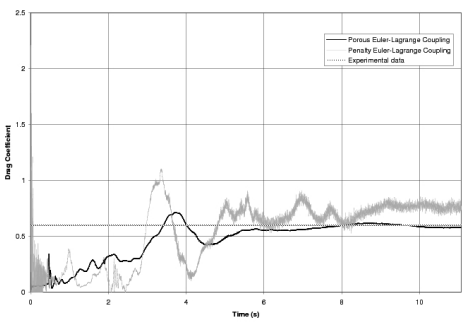

Figure 6 Drag Force Time History Data

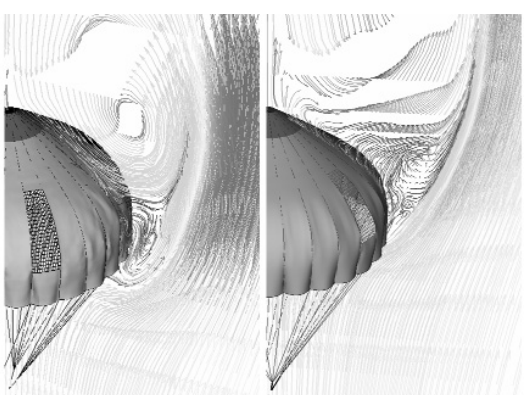

WITHOUT PERMEABILITY *WITH PERMEABILITY*

Figure 7 Visualization of the permeability effect

5. CONCLUSIONS

The combination of bluff body aerodynamics and a highly deformable structure, fabricated from a porous media, creates a truly unique and multifaceted environment. To appropriately simulate, and therefore understand and predict, this behavior requires an accurate method of assessing this complex relationship. This paper has provided a description of the implementation and validation of the porous Euler-Lagrange coupling algorithm for a transient dynamic finite element method. It has also discussed the importance of such a development to the parachute engineer and the future of parachute design. Numerical results have been shown to provide excellent correlation with actual test data, providing an authentic capability to model parachutes fabricated from permeable fabrics. The prospective goals of this ongoing research are to incorporate the effect of fluid viscosity and particularly density changes during parachute flight. This will enable extremely high altitude and interplanetary aerodynamic decelerators to be evaluated over a range of conditions. Also of interest is the influence of fabric loading on porosity and the subsequent change in permeability.

REFERENCES

1. Spahr, H.R., Wolf, D.E., Theoretical analysis of wake-induced parachute collapse, *7th AIAA Aerodyn. Decelerator and Balloon Technol. Conf.*, 1981, pp.81-1922
2. Stein, K., Benney, R., Kalro, V., Tezduyar, T.E., Leonard, J., Accorsi, M., Parachute fluid-structure interactions: 3-D Computation, *Computer Methods in Applied Mechanics and Engineering*, 2000, 190, pp.373-386.
3. Stein, K., Benney, R., Tezduyar, T.E., Potvin, J., Fluid-structure interactions of a cross parachute: Numerical simulation, *Computer Methods in Applied Mechanics and Engineering*, 2001, 191, pp.673-687.
4. Stein, K., Benney, R., Tezduyar, T.E., Leonard, J.W., Accorsi, M., Fluid-structure interactions of a round parachute: Modeling and simulation techniques, *Journal of Aircraft*, 2001, 38, pp.800-808.
5. Rosenhead, L., The formation of vortices from a surface of discontinuity, *Proc. Royal Society*, 1931, 134, pp.170-192.
6. Chorin, A.J., Numerical study of slightly viscous flow, *J. Fluid Mechanics*, 1973, 57, pp.785-796.
7. Peskin, C.S., The immersed boundary method, *Acta Numerica*, 2002, 11, pp. 479-517.
8. Kim, Y., Peskin, C.S., 2-D Parachute Simulation by the Immersed Boundary Method, to appear in *SIAM Journal on Scientific Computing*, 2006.
9. Kim, Y., Peskin, C.S., 3-D Parachute Simulation by the Immersed Boundary Method, submitted to *SISC*.
10. Benson, D., Eulerian-Lagrangian Coupling in Finite Element calculations with applications to machining, *Emerging Technology in Fluids, Structures, and Fluid-Structure Interactions - 2004, Volume 2*, July 25-29 2004, San Diego, California USA, PVP-Vol.485-2.
11. Aquelet, N., Souli, M., Olovsson L., Euler Lagrange Coupling with Damping Effects: Application to Slamming Problem, *Comput. Methods Appl. Mech. Engrg.*, 2005, CMA5874, 195(1-3), pp.110-132.
12. Strickland, J.H., Prediction method for unsteady axisymmetric flow over parachutes, *J. Aircr.*, 1994, 31(3), pp.637-643.
13. Higuchi, H., Balligand, H., Strickland, J.H., Numerical and experimental investigations of the unsteady axisymmetric flow over a disk, *Vortex Methods for Engineering Applications*, Albuquerque. NM, 1995, pp.219-291.
14. Sarpkaya, T., Lindsey, P.J., Unsteady flow about porous cambered plate, *J. Aircr.*, 1991, 28(8), pp.502-508.
15. Sundberg, W. D., PRONTO2D/VPARA Coupling, *International Sandia National Laboratories Memorandum*,W. P. Wolfe, January, 1999.
16. Taylor, L.M., Flanagan, D.P., PRONTO 2D, A Two-Dimensional Transient Solid Dynamics Program, *Sandia National Laboratories*, Albuquerque, New Mexico, March 1987, SAND86-0594.

17. Strickland, J. H., Homicz, G. F., Porter, V. L., Gossler, A. A., A 3-D Vortex Code for Parachute Flow Predictions: VIPAR Version 1.0, *Sandia National Laboratories*, Albuquerque, New Mexico, July 2002, SAND2002-2174.

18. Donea, J., An arbitrary Lagrangian-Eulerian finite element method for transient fluid-structure interactions. *Computational Mechanics*, 1982, 33 pp.689-723

19. Farhat, C., Lesoinne, M., Maman, N. , Mixed explicit/implicit time integration of coupled aeroelastic problems: three-field formulation, geometric conservation and distributed solution. *Int. Journal for Num. Meth. In Fluids*, 1995, 21, pp.807-835.

20. Cruz, J. R., Mineck, R. E., Keller, D. F., Bobskill, M. V., Wind Tunnel Testing of Various Disk-Gap-Band Parachutes, *17th AIAA Aerodynamic Decelerator Systems Technology Conference and Seminar*, Monterey, CA, May 19-22, 2003, AIAA 2003-2129.

21. Ergun, S., Fluid Flow Through Packed, *Chem. Eng. Prog.*, 1952, 48(2), pp.89-94.

22. Benson, D.J., Computational methods in Lagrangian and Eulerian hydrocodes, *Comp. Meth. Appl. Mech. Engrg.*, 1992, 99(2), pp.235-394.

23. Belytschko, T., Lin, J., Tsay, C.S., Explicit algorithms for nonlinear dynamics of shells, *Comp. Meth. Appl. Mech. Engrg.*, 1984, 42, pp.225-251.

24. Hughes, T.J.R., Liu, W.K., Zimmerman, T.K., Lagrangian Eulerian finite element formulation for viscous flows, *Comp. Meth. Appl. Mech.* Engrg., 1981, 21, pp.329-349.

25. Souli, M., Ouahsine, A., Lewin, L., ALE and Fluid-Structure Interaction problems, *Comp. Meth. Appl. Mech. Engrg.*, 2000, 190, pp.659-675.

26. Belytschko, T., Liu, W.K., Moran, B., *Nonlinear Finite Elements for Continua and Structures*, John Wiley & Sons, LTD, 2001.

27. Van Leer, B., Towards the Ultimate Conservative Difference Scheme.IV. A New Approach to Numerical Convection, *Journal Computational Physics*, 1977, 167, pp.276-299.

28. Hughes, T.J.R., Liu, W. K., Nonlinear Finite Element Analysis: Part I. Two-Dimensional Shells, *Comp. Meth. Appl. Mech. Engrg.*, 1981, 27, pp.167-181.

29. Knacke, T.W., *Parachute Recovery Systems Design Manual*, Para-Publishing, Santa Barbara, CA, 1992.

30. Belytschko, T., Neal, M.O., Contact-impact by the pinball algorithm with penalty, projection, and Lagrangian methods, *Proc. Symp. on Computational Techniques for Impact, Penetration, and Performation of Solids*, ASME, New York, NY, 1989, AMD-Vol. 103, pp.97-140.

31. Tutt, B., The use of LS-DYNA to Assess the Performance of Airborne Systems North America Candidate ATPS Main Parachutes, *AIAA Aerodynamic Decelerator Systems Conference*, 2005.